Macroporous hydrogels based on 2-hydroxyethyl methacrylate. Part 5: Hydrolytically degradable materials

**Martin Přádný · Jiří Michálek · Petr Lesný ·
Aleš Hejčl · Jiří Vacík · Miroslav Šlouf · Eva Syková**

Abstract Macroporous hydrogels based on 2-hydroxyethyl methacrylate, 2-ethoxyethyl methacrylate and *N*-(2-hydroxypropyl)methacrylamide, methacrylic acid and [2-(methacryloyloxy)ethyl]trimethylammonium chloride crosslinked with *N,O*-dimethacryloylhydroxylamine were prepared. Hydrogels were degraded in a buffer of pH 7.4. Completely water-soluble polymers were obtained over time periods ranging from 2 to 40 days. The process of degradation was followed gravimetrically and by optical and electron microscopy. *In vivo* biological tests with hydrogels based on copolymers of 2-ethoxyethyl methacrylate/*N*-(2-hydroxypropyl)methacrylamide were performed.

Introduction

The importance of biomaterials has dramatically increased in recent years, and the number of polymer applications in medicine and pharmacology continues to grow [1, 2]. In addition to the industrial production of soft and hard contact lenses [3, 4], polymers are used as intraocular lenses [5], implants (in otorhinolaryngology [6], surgery [7], gynaecology [8], urology [9] and neurology [10]) and as carriers of living cells in the treatment of burns, decubitus, and other skin injuries [11, 12]. Polymers are also used in ointments [13], as drug carriers [14], blood extenders [15], synthetic emboli and other surgery materials [16] (sewing and dressing materials), injection syringes, and as a construction material [17]. These and a number of other polymer applications in medicine and pharmacy result in numerous and often antagonistic requirements for polymers and their properties in terms of their technology, chemistry and biology. In every case, it is necessary to fulfil the primary requirements of material stability and good biocompatibility. Synthetic hydrogels partly allow the optimization of their properties in dependence on their structure.

For many purposes, it is appropriate to modify the materials so that they degrade, after some time in contact with living tissue, to water-soluble substances, which can then be eliminated by the organism. A number of such materials are used, e.g., for targeted drugs or in the therapy of central nervous tissue at a site where, without their implantation, only a pseudocyst would otherwise form [18–21].

In previous studies we reported the synthesis and physicochemical characterization of hydrolytically non-degradable hydrogels based on copolymers of 2-hydroxyethyl methacrylate with sodium methacrylate [22] or [2-(methacryloyloxy)ethyl]trimethylammonium chloride [23], to be utilized as implants, e.g. in the central nervous system. The materials were further studied from the viewpoint of the sorption and desorption of proteins and, at the same time, their interaction with living tissue was examined. On the basis of a number of positive results published previously [22–24], we decided to abandon the successful but non-degradable and hence ultimately unsuitable model materials described above and to replace them with hydrophilic polymers crosslinked with a hydrolytically

M. Přádný (✉) · J. Michálek · J. Vacík · M. Šlouf
Institute of Macromolecular Chemistry, Academy of Sciences of the Czech Republic, 162 06 Prague 6, Czech Republic
e-mail: pradny@imc.cas.cz

J. Michálek · J. Vacík
Center for Cell Therapy and Tissue Repair, Charles University, 150 06 Prague 5, Czech Republic

P. Lesný · A. Hejčl · E. Syková
Center for Cell Therapy and Tissue Repair, Charles University, 150 06 Prague 5, Czech Republic, and Institute of Experimental Medicine, Academy of Sciences of the Czech Republic, 142 20 Prague 4, Czech Republic

degradable crosslinker, *N,O*-dimethacryloylhydroxylamine, which has been studied previously [25–27]. The main reason for the use of degradable hydrogels is to enable their spontaneous dissolution after cell proliferation in the implant, while the tissue formed in conjunction with the supporting action of the hydrogel is retained. Using specific components in the polymerization mixture, we were able to prepare suitable macroporous structures with the expected parameters; the rate of hydrogel degradation can be set over a relatively wide time range. We then implanted selected degradable hydrogels into the spinal cords of laboratory rats and left them there for 30 days in order to determine the degradation rate of the hydrogels *in vivo*.

Experimental

Chemicals

N-(2-hydroxypropyl)methacrylamide (HPMA) was prepared by the methacryloylation of 2-hydroxypropylamine [28], and *N,O*-dimethacryloylhydroxylamine (DMHA) by the methacryloylation of hydroxylamine [25–27]. 2-hydroxyethyl methacrylate (HEMA) (Rohm) was used after shaking (10 times) with a mixture water/hexane (1:1) and drying with anhydrous sodium sulfate. The content of ethylene dimethacrylate (EDMA) was 0.07% (GPC), purity 99.3%. Methacrylic acid (MA) and 2-ethoxyethyl methacrylate (EOEMA) were used after distillation. [2-(Methacryloyloxy)ethyl]trimethylammonium chloride (MOETACl) was prepared by the quaternization of 2-(dimethylamino)ethyl methacrylate with methyl iodide, the conversion of the product into the Cl form on a column with the strongly basic ion exchanger IRA 402 (Fluka) in Cl cycle and crystallization from a water/acetone mixture [23].

Hydrogels

Macroporous hydrogels were prepared by crosslinking radical polymerization of the monomers, crosslinker (DMHA), poly(ethylene glycol) 400 (PEG) and fractionated sodium chloride particles (0–30 μm, 30–50 μm and 50–90 μm) with azobis(isobutyronitrile) (AIBN) at 80°C for 8 h. After polymerization, sodium chloride and PEG were removed by washing (10 times) in citrate buffer, pH 3:

citric acid	8.406 g
sodium hydroxide	0.846 g
sodium chloride	7.217 g
Water	to 1 l

Details of the hydrogel preparation in the polymerization chamber of a special device have been described previously [22, 23].

Compositions of the hydrogels were:

HEMA/HPMA	0, 13, 23 and 34% HEMA by weight
HEMA/MOETACl	23, 60, 81 and 100% HEMA by weight
HEMA/MA	21, 57 and 71% HEMA by weight
EOEMA/HPMA	21, 29, 43 and 50% EOEMA by weight

The content of the crosslinker (DMHA) was 2.7% by weight, relative to the monomers.

Degradation

As previously noted, we intend to use these hydrolytically degradable hydrogels as implants in nervous tissue, therefore, all experiments were made under physiological conditions, i.e. at pH 7.4, temperature 37°C and at the same ionic strength as in physiological solution. The composition of the pH 7.4 buffer was:

potassium dihydrogen phosphate	6.805 g
sodium hydroxide	1.160 g
sodium chloride	5.282 g
water	to 1 l

A sample of the hydrogel was kept at pH 3 and 37°C for 24 h, washed four times with pH 7.4 buffer (2 h) (weight m_0), and weighed in a swollen state in one-day intervals (weight m). The relative change in weight was calculated as

$$\delta = (m - m_0)/m_0$$

Microscopy

The degradation of the hydrogels as a function of time was also followed by microscopy. Two microscopic techniques were used: light microscopy (LM) was employed to monitor the gradual dissolution of the hydrogels in buffer (pH 7.4), while low-vacuum scanning electron microscopy (LVSEM) made it possible to follow changes in the supramolecular structure of the hydrogels

Sample preparation

Fresh hydrogel was prepared and kept in a refrigerator at pH 4. The hydrogel, still immersed in buffer, was cut with a sharp blade into two pieces: the first, a sample for LM, was a small cube ($\approx$0.5 cm), the other was used for LVSEM. On the first day of microscopic observations (time = 0), the hydrogel was heated to 37°C and transferred into pH 7.4 buffer.

Light microscopy

The LM sample was kept at 37°C and pH 7.4 and observed daily with a light microscope (Nikon) equipped with a digital camera (DXM 1200, Nikon). During observation, the

sample was placed in a Petri dish, completely immersed in the buffer. Side illumination was used to increase contrast, and a moderate magnification was chosen so that the entire sample could be contained in a single micrograph. Light microscopy observations were performed every day, exactly 24 h apart, until the entire sample was degraded, i.e. until the sample dissolved completely.

Low-vacuum scanning electron microscopy

A small part of the sample for LVSEM was cut off using a sharp blade while the sample was still immersed in buffer. This small part was flash-frozen in liquid nitrogen and fixed to the heating stage of an LVSEM microscope (AquaSEM, Tescan, Czech Republic) with a small drop of water. The freshly cut surface was observed in the microscope after sublimation of ice, as described in more detail in our previous studies [22–24].

Image analysis

A series of LM microphotographs underwent image analysis, which was performed using the program Lucia (LIM, Czech Republic). The area of the sample, S, in mm^2 was determined directly for each image. The approximate length of the cube edge was calculated as $a = \sqrt{S}$ and the approximate volume of the cube was calculated as $V = a^3$. As the sample swells during degradation, relative increases in sample length ($\Delta a = (a - a_0)/a_0$), area ($\Delta S = (S - S_0)/S_0$) and volume ($\Delta V = (V - V_0)/V_0$) must be increasing functions of time, associated with the degree of hydrolysis.

Implantation

For testing the behaviour of the hydrogels *in vivo*, blocks of EOEMA/HPMA hydrogels with 21% EOEMA were implanted into hemisections formed in the spinal cords of laboratory brown rats. Females Wistar rats ($n = 4$) were anesthesized with isofluoran; a laminectomy was then performed at the Th6-Th7 level. The dura mater was cut along the medial line, and a 2-cm block of spinal cord tissue was removed on the right-hand side of the medial line using sharp scissors.

A $2 \times 2 \times 2$ mm hydrogel block was incubated in phosphate buffer pH 7.4 for 20 min and then implanted into a hemisection. The dura mater was sutured with Prolen 8/0 (Ethicon), and the muscles and subcutaneous tissue were sutured in anatomical layers. After surgery, the animals were administered antibiotics and analgetics and left to recover on a heated pad. After 30 days the animals were sacrificed and the spinal cords processed histologically (Hematoxylin—Eosin and Cresyl Violet staining) and immunohistochemi-

cally using antibodies directed against neurofilaments and astrocytes (anti-NF160 and anti-GFAP, respectively).

Results and discussion

Kinetics of degradation

As published previously [25], dimethacryloylated hydroxylamine is unstable in solution at pH > 6, undergoing hydrolysis. If the crosslinker is incorporated into a three-dimensional network, a linear polymer is formed after hydrolysis that bears carboxylic and amino groups at the original junction points. We made use of this fact for the preparation of hydrolytically degradable macroporous hydrogels by a technique described in our previous papers [22, 23].

As starting materials for degradable hydrogels, monomer pairs were selected in which one of the pair is strongly hydrophilic and the other is less hydrophilic, so that its homopolymer does not dissolve in water. The addition of the less hydrophilic comonomer makes it possible to prolong the hydrogel degradation time. Hydrogels consisting of a water-soluble homopolymer dissolve in water, degrading very fast (in 2–5 days), whereas hydrogels containing a water-insoluble homopolymer cannot degrade. One of the goals of the present work was to develop a hydrogel set with adjustable degradation times. As pairs of medium- and strong-hydrophilic comonomers, we selected HEMA in combination with an uncharged comonomer (HPMA), a positively charged comonomer (MOETACl) or a negatively charged (MA) comonomer. In addition, we tested the neutral EOEMA/HPMA pair, which, in contrast to HEMA, does not contain any residual non-degradable crosslinker (ethylene dimethacrylate, EDMA).

The degradation kinetics of the synthesized macroporous hydrogels expressed as the relative weight change of the samples (change in hydrogel weight relative to initial weight) are shown in Figs. 1–3.

At the first stage, when the crosslinks between chains break, the density decreases and hydrogel swelling increases.
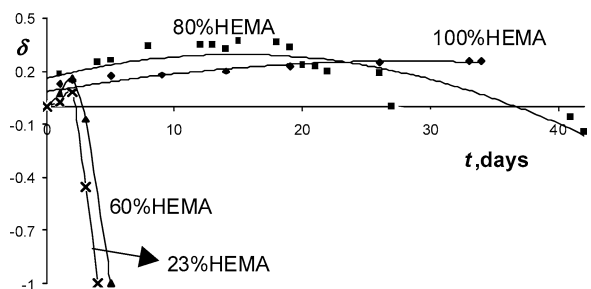

Fig. 1 Dependence of the relative weight of macroporous hydrogels (HEMA/HPMA) on time. NaCl particles 30–50 μm, pH 7.4, 37°C, DMHA content 2.7% (relative to the monomers).
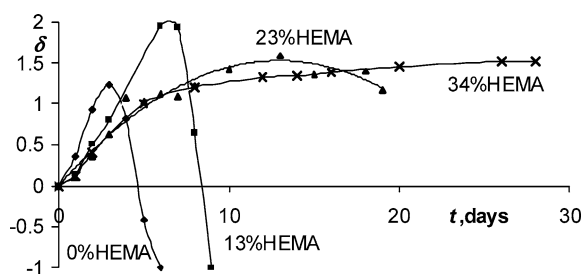
Fig. 2 Dependence of the relative weight of macroporous hydrogels (HEMA/MOETACl) on time. NaCl particles 30–50 μm, pH 7.4, 37°C, DMHA content 2.7% (relative to the monomers).
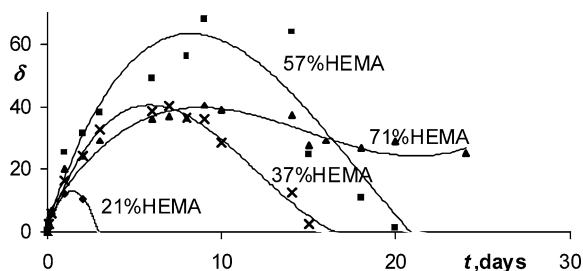

Fig. 3 Dependence of the relative weight of macroporous hydrogels (HEMA/MA) on time. NaCl particles 30–50 μm, pH 7.4, 37°C, DMHA content 2.7% (relative to the monomers).

At the moment when the network density is so low that the copolymer becomes soluble in water, the kinetic curve shows a maximum, the hydrogel dissolves and its relative weight decreases. At the moment when $\delta = -1$, the whole volume of the hydrogel is dissolved.

In every case, the curves shown in Figs. 1–3 (and also 4–6) resulted from a combination of two antagonistic processes. First, swelling starts when the hydrogel is moved from a buffer of pH 3 to a solution with a pH of 7.4, and the weight of the sample increases. Second, the rate of cleavage of the hydrolysable crosslinks simultaneously increases with increasing swelling, and subsequently the weight of the sample decreases.

As can be seen in Fig. 1, the degradation kinetics for hydrogels with 23% and 60% HEMA are similar and the time necessary for cleavage is very short (4–5 days). In contrast, hydrogels with a HEMA content of 80% degrade slowly (43 days). The explanation for the different shapes of the curves is based on the large difference between poly(HPMA) and poly(HEMA) swelling. Copolymers of HPMA with a low HEMA content are swollen to such an extent that the hydrolysis of degradable crosslinks is fast and similar over a wide range of HEMA contents (23% to 60%). The influence of a higher HEMA content can be seen in the HPMA/HEMA copolymer containing 80% HEMA. The swelling is low, and the cleavage rate decreases. In addition, the number of non-degradable crosslinks formed by EDMA, the residual crosslinker from HEMA, increases with increasing HEMA content. EDMA crosslinks prolong the splitting time of the

gel so that the curve for pure poly(HEMA) shows that a swelling equilibrium was established.

The effect of electrical charge on the course of the degradation process is apparent from Figs. 1–3. The lowest increase, δ, was seen with hydrogels bearing a positive charge, in which swelling increased by 20% at the maximum (Fig. 2). At the same time the degradation proceeded very fast (3–4 days), as in the hydrogels with comparatively high HEMA contents (60%). Hydrogels with higher contents of HEMA cannot hydrolytically degrade as they contain minute amounts (0.07%) of the hydrolytically stable crosslinker, ethylene dimethacrylate, which cannot be completely removed from the monomer. Uncharged hydrogels showed a somewhat greater degree of swelling (150–200%) during their degradation (Fig. 1). At the same time, the time period during which the hydrogels completely degraded was a little longer than with the positively charged hydrogels (6–9 days); so that the HEMA content must be very low (less than 13%). At higher HEMA contents, the hydrogels no longer degrade. The differences between hydrogels with a positive charge and those without charge can be ascribed to the extremely strong hydrophilicity of the MOETACl comonomer. Although both types of hydrogels contain a crosslinker that cannot degrade, the strong hydrophilicity of MOETACl can obviously result in the breakage of crosslinks and thus the dissolution of the copolymer. At the same time, hydrogels with positive charges are greatly swollen and hence a further increase in swelling, expressed as δ, is not so noticeable as for the hydrogels without charge. The greatest swelling (4000–6000%) was observed for hydrogels bearing negative charges (Fig. 3). This is not surprising: at the beginning of the degradation process, the hydrogel is swollen only very little as it contains only very few dissociated carboxylic groups. Over the course of degradation at pH 7.4, these groups dissociate, the hydrogel becomes more hydrophilic and its swelling increases. At the same time, the HEMA content in the portion of the gel that can still degrade is relatively high, comparable with the hydrogels containing positive charges; however, the degradation time is longer.

The curves in Fig. 3 reflect the ratio between the cleavage rate (weight loss) and the swelling rate (weight increase). Due to this fact, the swelling apparently increases with increasing HEMA content (21%–57%), but the real cause is the slowing down of the degradation rate due to increasing proportion of the non-degradable crosslinker EDMA. The 71% HEMA curve serves as proof of this statement; the HEMA content is so high that the degradation process is very slow and after approximately 20 days swelling equilibrium was established. Simultaneously, the content of strongly swollen comonomer (29% MA) is so low that the swelling maximum does not reach the values observed in copolymers with higher concentration of MA.
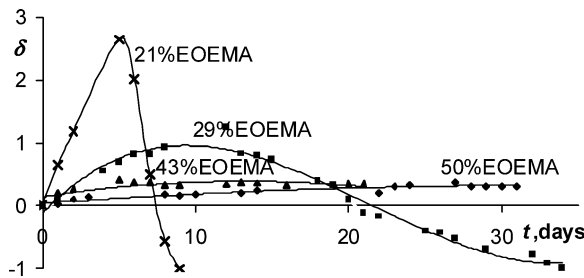
Fig. 4 Dependence of the relative weight of macroporous hydrogels (EOEMA/HPMA) on time. NaCl particles 30–50 μm, pH 7.4, 37°C, DMHA content 2.7% (relative to the monomers).

The degradation kinetics of hydrogels with the low-hydrophilic comonomer EOEMA in combination with the hydrophilic uncharged comonomer HPMA are shown in Fig. 4.

In contrast to 2-hydroxyethyl methacrylate, 2-ethoxyethyl methacrylate does not contain any hydrolytically non-degradable crosslinker and is noticeably more hydrophobic. Thus, the EOEMA/HPMA copolymers are not affected by any residual non-degradable crosslinker, in contrast to HEMA/MOETACl or HEMA/MA copolymers. We were therefore interested in examining how this affects the degradation kinetics. It follows from Fig. 4 that hydrogel degradation proceeds noticeably slower at hydrophobic monomer contents below 30%, considerably slower than for HEMA-based gels. At the same time, the kinetic curves show maxima comparable with the curves for HEMA/HPMA hydrogels. The maximum amount of the more hydrophobic comonomer in the EOEMA/HPMA hydrogels, when the degradation still proceeds, is higher compared with that in the HEMA/HPMA hydrogels, due to the absence of a hydrolytically non-degradable crosslinker. The low solvation of polymer chains containing hydrophobic EOEMA units compared with HEMA chains prolongs the degradation of the crosslinker, as follows from a comparison of Figs. 1 and 4.

The curves in Fig. 4 again reflect the combination of two processes: swelling and degradation. As a result, we observed maximal swelling and rapid degradation in the copolymers with low contents of hydrophobic EOEMA. The swelling is lower with increasing EOEMA content, while at the same time the curve becomes (as expected) flatter with increasing EOEMA content, due to limited access of solvent to the degradable crosslinks, so that copolymers with the EOEMA content greater than 43% are practically non-degradable.

The degradation kinetics of macroporous hydrogels in dependence on the NaCl particle size used in their synthesis is shown in Fig. 5. The pore size and distribution approximately correspond to the NaCl particle size, as described earlier [22, 23]. Due to very poor mechanical properties of the hydrogels, mercury or nitrogen porosimetry could not be used. The kinetic curves show more noticeable maxima when smaller
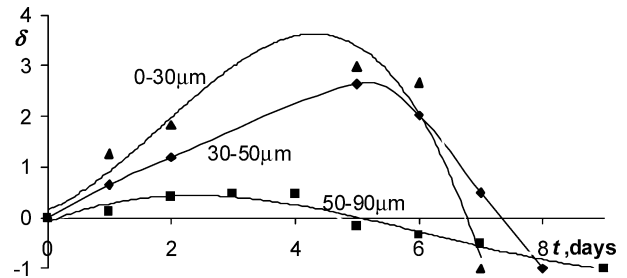
NaCl particles were used, and the time required for complete degradation of the hydrogels moderately increased.

This observation is a consequence of the increase in the total pore surface area with increasing NaCl particle size [22, 23]; the hydrolytic agent has easier access to the crosslinks between macromolecules and thus the time required for degradation decreases. Due to the fact that the thickness of the walls between pores increases with decreasing NaCl particle size, hydrogel swelling increases more in the course of degradation and the maxima of δ on the graph δ versus t are more pronounced.

The dependence of degradation kinetics on the crosslinker content is shown in Fig. 6. It follows from the graph that the time required for the degradation of a hydrogel prolongs with increasing DMHA concentration and the maxima on the curves become less pronounced. A greater crosslinker content causes a longer hydrogel degradation time. At the same time, a higher network density leads to lower swelling, which corresponds to less pronounced maxima for the kinetic curves.

Microscopy and image analysis

Degradation of the hydrogels was accompanied by their swelling, as documented by LM (Fig. 7A and B). We used EOEMA/HPMA hydrogels containing 21% EOEMA
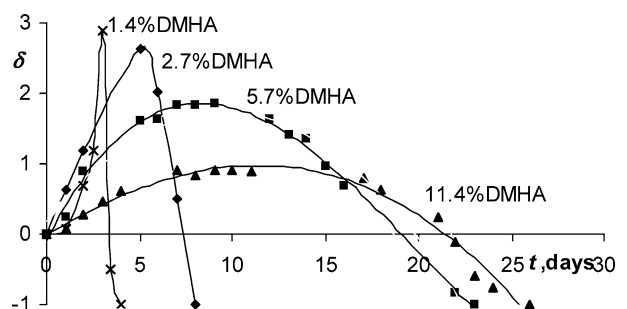

Fig. 5 Dependence of the relative weight of macroporous hydrogels (EOEMA/HPMA) on time for different porosities and average particle sizes of NaCl. pH 7.4, 37°C, DMHA content 2.7% (relative to monomers).

Fig. 6 Dependence of the relative weight of macroporous hyrdogels (EOEMA/HPMA) on time for different amounts of crosslinker. NaCl particles 30–50 μm, pH 7.4, 37°C, DMHA content 2.7% (relative to the monomers).
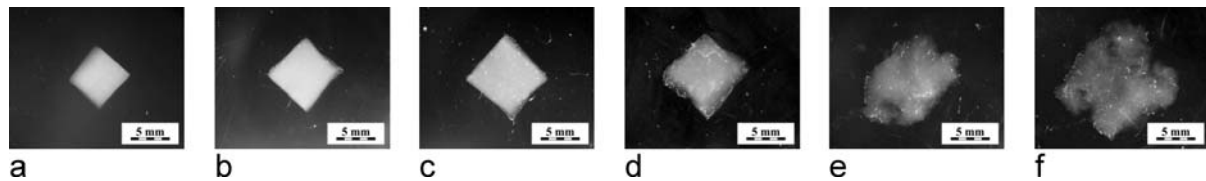
Fig. 7 (A) Degradation of EOEMA/HPMA hydrogels with 21% EOEMA, followed by LM. The first microphotograph (a) shows a small cube of hydrogel immediately after immersion in buffer at pH 7.4. The following microphotographs show the sample after (b) one, (c) two, (d) three, (e) four and (f) six days.
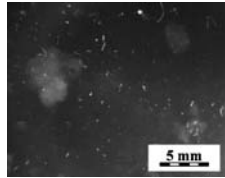

Fig. 7 (B) LM microphotograph showing a hydrogel after seven days at pH 7.4 and 37°C. On day eight the hydrogel was completely degraded and thus could not be observed.

crosslinked with 2.7% DMHA. Swelling started immediately after immersing the sample into pH 7.4 buffer. LM photomicrographs suggest that the rate of degradation slightly increases with time. This was confirmed by image analysis (Fig. 8), in which the relative change of the cube edge, Δa, cube wall, ΔS, and cube volume, ΔV, were plotted as functions of time. The calculation of Δa, ΔS and ΔV is described in the Experimental section. All three functions are associated with the degree of swelling, all increase and their slopes rise over time, in particular ΔV.

The determination of ΔV by image analysis is inherently prone to error, which arises from the increasing degree of hydrogel degradation. The calculation of ΔV is based on the assumption that the hydrogel sample, originally cubic in shape, swells evenly in all three dimensions so that the cube evenly expands. In reality, the structure collapses at advanced stages of degradation and the cube flattens. Hence the third dimension of the cube shrinks, which the calculation does not take into account, resulting in an overestimation of ΔV, which increases with increasing degradation of the hydrogel. After six days, image analysis was no longer feasible as the hydrogels reached an advanced stage of degradation and a maximum analogous to that on the δ vs. time curves was not visible on the ΔV (ΔS, Δa) curves (Fig. 4).
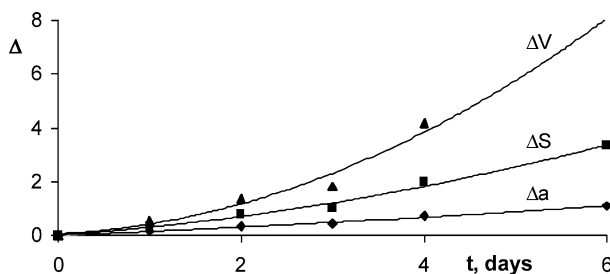

Fig. 8 Degree of swelling calculated from LM microphotographs.

LM affords an overall view of the degradation, whereas LVSEM provides an opportunity to observe changes in the supramolecular structure (Fig. 9). In the beginning, the samples exhibited a distinct structure, i.e. thin and sharp polymer walls between the pores (Fig. 9a). In the course of time, the walls swell and later dissolve. As a result, the sample structure becomes more and more diffuse and fuzzy (Fig. 9b–d). This microscopic swelling is in accord with the macroscopic swelling observed with LM at lower magnification (Fig. 7). After four days of degradation the samples were so soft that they could not be transferred into liquid nitrogen without being completely destroyed.

Results *in vivo*

For biological tests *in vivo*, EOEMA/HPMA hydrogels with 21% EOEMA, crosslinked with 2.1% DMHA, were used. The hydrogels were cut into $2 \times 2 \times 2$ mm pieces and sterilized with UV light. Although the degradation time for the hydrogels *in vitro* was 8 days (Fig. 4), complete degradation of the hydrogels was not achieved *in vivo*. We found only a minimal sterile inflammatory reaction in the surrounding tissue and no foreign body reaction, therefore we conclude that these particular hydrogels are biocompatible. The sterile inflammatory reaction was probably due to the tissue damage during the surgery. In spinal cord defects filled with hydrogel, tissue was formed containing predominantly connective tissue elements (Fig. 10). The tissue reaction was as follows: in the marginal layer of the hydrogel, low-density connective tissue with an arterial network was present, reminiscent of the structure of the original macroporous hydrogel. We found polymer traces only in macrophages in the form of inclusions. It is of interest that neurofilaments grew through this layer. The defect center was filled with dense tissue containing only disorganized hydrogel residues and dense cell elements, without the presence of arteries or macrophages. The basic structure of the hydrogel was no longer apparent.

At physiological pH, the hydrogel probably degrades throughout the entire implanted block. In the periphery, which was in tight contact with the spinal cord tissue and where neovascularization occurred, the hydrogel was replaced with low-density connective tissue. Hydrogel degradation also occurred, but the polymer was not removed
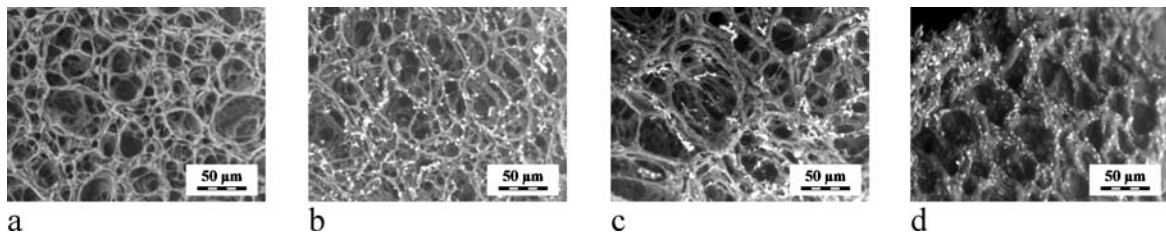
Fig. 9 Degradation of a hydrogel followed by LVSEM. The microphotograhs show the sample (a) immediately after immersion in pH 7.4 buffer and after remaining in the buffer for (b) one, (c) two and (d) three days.

Fig. 10 Histological investigation of EOEMA/HPMA hydrogels with 21% EOEMA, implanted for 30 days in a hemisected rat spinal cord. The hydrogel implant originally matched the width of the spinal cord lesion. A. The lesion site shows minimal sterile inflammation in the surrounding tissue and in the peripheral and central regions of the lesion. Scale bar = 500 μm. B. The vascularised tissue in the peripheral region of the lesion contains a large number of macrophages. Scale bar = 50 μm. C. The dense tissue in the center of the lesion. Scale bar = 50 μm. D. NF160-positive neurofilaments in the peripheral region of the lesion. Scale bar = 50 μm.
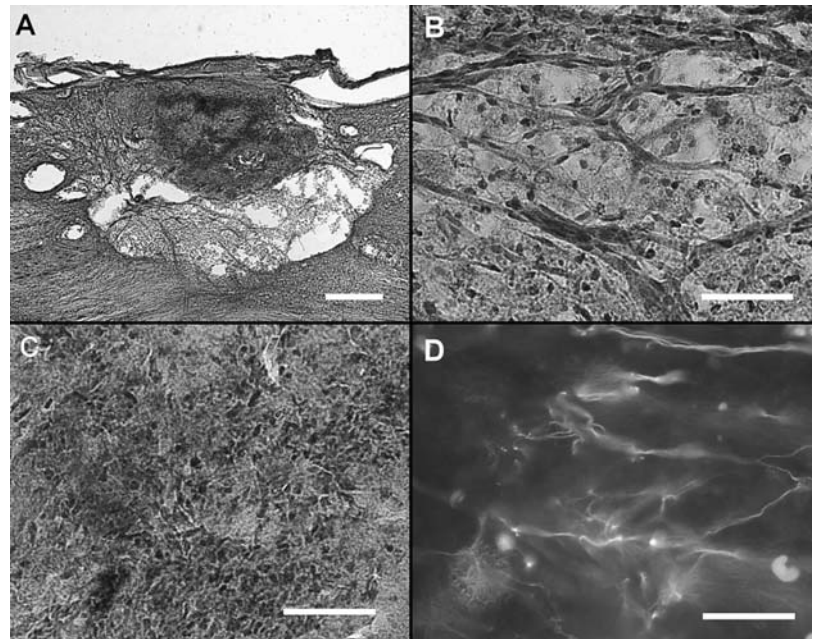
sufficiently quickly to avoid its replacement by tissue of lower quality, which did not contain neurofilaments.

These *in vivo* experiments show that macroporous hydrolysable hydrogels based on EOEMA/HPMA are suitable candidates for implantation into tissue defects in the central nervous system. In assessing hydrolysable hydrogels *in vivo*, it is necessary to take into consideration not only the hydrolysis rate, but also the rate of hydrogel removal from the lesion site. In future assessments of materials designed for the therapy of spinal cord injuries, it will be important to concentrate on appropriate tuning of the hydrolysis rate so that the formation of new tissue can occur throughout the bulk of the hydrogel.

References

1. F. H. SILVER and R. W. JOHNSON, "Biomaterials, Medical Devices and Tissue ngineering: An Integrated Approach" (Chapman & Hall, London, 1994).
2. M. SEFTON, New Biomaterials, The 7th New Jersey Symposium on Biomaterials Science, New Brunswick (2004).
3. N. EFRON, "The International Contact Lens Year Book" (W.B. Saunders Company Ltd., 1993).
4. N. EFRON, "Contact Lens Practice" (Butterworth—Heinemann, New Delhi, 2002), p. 76.
5. R. G. MARTIN, J. P. GILLS and D. R. SANDERS, "Foldable Intraocular Lenses" (Slack Inc., NJ, USA, 1993), Section II and III.
6. M. ZIGNANI, S. F. BERNATCHEZ and T. LE MINH, *J. Biomed. Mater. Res.* **39** (1998) 277.
7. V. OLIVER, N. FAUCHEUX and P. HARDOUIN, *Drug Discovery Today* **9** (2004) 803.
8. T. E. J. IND, J. C. SHELTON and J. H. SHEPHERD, *Br. J. Obstetrics Gynaecol.* **108** (2001) 1013.

9. L. ŠEFC, M. PŘÁDNÝ, J. VACÍK, J. MICHÁLEK, C. POVÝŠIL, I. VÍTKOVÁ, M. HALAŠKA and V. ŠIMON, *Biomaterials* **23** (2002) 3711.

10. P. LESNÝ, J. De CROOS, M. PŘÁDNÝ, J. VACÍK, J. MICHÁLEK, S. WOERLY and E. SYKOVÁ, *J. Chem. Neuroanat.* **23** (2002) 243.

11. K. SMETANA, B. DVOŘÁNKOVÁ, M. JELÍNKOVÁ, J. MICHÁLEK and J. VACÍK, *J. Mater. Sci.: Mater. Med.* **8** (1997) 587.

12. B. DVOŘÁNKOVÁ, Z. HOLÍKOVÁ, J. VACÍK, R. KÖNIGOVÁ, Z. KAPOUNKOVÁ, J. MICHÁLEK, M. PŘÁDNÝ and K. SMETANA, *Int. J. Dermatol.* **42** (2003) 219–223.

13. J. S. AHN, H. K. CHOI and M. K. CHUN, *Biomaterials* **23** (2002) 1411.

14. K. ULBRICH, M. PECHAR, T. ETRYCH, M. JELÍNKOVÁ, M. KOVÁŘ and B. ŘÍHOVÁ, *Mater. Struct.* **10** (2003) 3.

15. K. Y. CHEN, J. F. KUO and C. Y. CHEN, *Biomaterials* **21** (2000) 161.

16. N. A. PEPPAS, "Hydrogels in Medicine and Pharmacy" (CRC Press, Boca Raton, 1986).

17. S. A. BERGER, W. GOLDSMITH and E. R. LEWIS, "Introduction to Bioengineering" (Oxford University Press, 1996).

18. S. W. KIM, *Polym. Mater. Sci. Eng.* **89** (2003) 178.

19. V. ŠKARDA and F. RYPÁČEK, *J. Bioact. Compat. Polym.* **12** (1997) 186.

20. S. WOERLY, D. DOAN, N. SOSA, J. VELLIS and A. ESPINOSA, *Int. J. Dev. Neurosc.* **19** (2001) 63.

21. H. DRNOVSKÁ, M. ŠLOUF and F. RYPÁČEK, "in Proceedings of the 40th IUPAC International Symposium on Macromolecules" (World Polymer Congress, Paris, 2004), p. 108.

22. M. PŘÁDNÝ, P. LESNÝ, J. FIALA, J. VACÍK, M. ŠLOUF, J. MICHÁLEK and E. SYKOVÁ, *Collect. Czech. Chem. Commun.* **68** (2003) 812.

23. M. PŘÁDNÝ, P. LESNÝ, K. SMETANA Jr., J. VACÍK, M. ŠLOUF, J. MICHÁLEK and E. SYKOVÁ, *J. Mater. Sci.: Mater. Med.* **16** (2005) 767.

24. J. MICHÁLEK, M. PŘÁDNÝ, A. ARTYUKHOV, M. ŠLOUF, J. VACÍK, K. SMETANA Jr., *J. Mater. Sci.: Mater. Med.* **16** (2005) 783.

25. K. ULBRICH, V. ŠUBR, P. PODPĚROVÁ and M. BUREŠOVÁ, *J. Controlled Release* **34** (1995) 155.

26. D. HORÁK and O. CHAIKIVSKYY, *J. Polym. Sci., Part A: Polym. Chem.* **40** (2002) 1625.

27. K. ULBRICH, V. ŠUBR, L. W. SEYMOUR and R. DUNCAN, *J. Controlled Release* **24** (1993) 181.

28. J. STROHALM and J. KOPEČEK, *Angew. Makromol. Chem.* **70** (1978) 109.